Glass and phase transitions in $(KBr)_{1-x}(KCN)_x$

A. Loidl and K. Knorr

Institut für Physik, Universität Mainz, D-6500 Mainz, Federal Republic of Germany

J. M. Rowe

Institute for Materials Research, National Bureau of Standards, Washington, D.C. 20234

G. J. McIntyre

Institut Max Laue–Paul Langevin, Boîte Postal 156X, F-38042 Grenoble Cédex, France

(Received 5 June 1987)

Results of a single-crystal neutron-diffraction study of the mixed molecular system $(KBr)_{1-x}(KCN)_x$ are presented. The crystal with a CN^- concentration $x = 0.65$ exhibits a ferroelastic transition from a plastic high-temperature phase of cubic symmetry to a low-temperature rhombohedral phase. The crystals with concentrations $x = 0.53$ and 0.57 undergo transitions into a quadrupolar glass state. In all the crystals investigated, the diffraction profiles near the transition temperatures are dominated by diffuse-scattering contributions. These diffuse intensities are due to random strains which are generated by the substitutional Br^- atoms acting as static impurity centers. The results demonstrate the importance of random strains for the order of the low-temperature state: A delicate balance between the rotation-translation coupling and the random strain fields determines the low-temperature phase. If the latter dominate, the elastic-order transition is suppressed and local order is frozen in. The temperature dependences of the diffuse scattered intensities are analyzed: Unusual line shapes and an unusual wave-vector dependence of the linewidths are found. In addition, the temperature dependence of Debye-Waller factors and of the orientational distribution of the CN^- molecules is studied in detail.

I. INTRODUCTION

The alkali-cyanide–alkali-halide mixed crystals $(MX)_{1-x}(MCN)_x$, where M is an alkali metal and X a halogen ion, continue to attract considerable attention because of the variety of phenomena that can be studied in these systems. Above a critical concentration x_c these crystals are model systems for ferroelastic phase transitions.[1-3] Below x_c they undergo transitions into a quadrupolar glass state.[4-6]

At room temperature all the alkali-cyanide–alkali-halide crystals exhibit a cubic phase where the high symmetry is established via a fast reorientational motion of the CN^- ions. On lowering the temperature the mixed crystals with concentrations $x \geq x_c$ undergo structural phase transitions from the high-temperature plastic phase into elastically ordered states, where the CN^- molecules are aligned and the center-of-mass lattice undergoes shear deformations. The mixed systems investigated so far exhibit an amazing polymorphism: ortho-rhombic, monoclinic, triclinic, and rhombohedral phases have been reported.[7-10] The structural phase transitions are driven by a strong rotation-translation coupling of molecular reorientations and T_{2g} shear strains.[1] As a consequence, the elastic constant c_{44} goes soft[11] as the transition temperature T_s is approached. It has been suggested that random strains play an important role in determining the structure of the low-temperature phase.[12] Finally, below the critical concentration, random strain fields suppress the phase transition and a new

low-temperature state, a quadrupolar glass, is observed. Recent theoretical work has shown that the coupling of random strains to the orientational degrees of freedom is responsible for the formation of the orientational glass.[13] The glass transition is indicated by cusps in the quadrupolar susceptibility.[13] Frequency-dependent anomalies in the elastic[4,6,14-18] and in the dielectric[6,19-21] susceptibilities have been observed. There is also experimental evidence that the dipolar (head-to-tail) and the quadrupolar (orientational) freezing temperatures differ.[18,21,22] In optical transmission experiments the glassy crystals remain transparent at all temperatures.[19] This has been taken as evidence that the overall symmetry of these crystals stays cubic. However, in diffraction experiments, an enormous broadening and anomalous line shapes of the diffraction lines at the glass transition temperature have been reported.[23,24] The low-temperature thermodynamic,[25] ultrasonic[26] and dielectric[27] properties are analogous to those found in canonical glasses and in amorphous systems.

The majority of investigations have been performed in KBr:KCN mixtures, where the Br^- ions randomly substitute the CN^- on the anion lattice. Pure KCN undergoes a cubic to orthorhombic ferroelastic transition at 168 K, followed by an antiferroelectric ordering transition at 83 K.[28] However, the low-temperature structure of $(KBr)_{1-x}(KCN)_x$ depends critically on the dilution with Br^- ions and below the critical concentration $x_c \simeq 0.6$ the ferroelastic transition is suppressed. For $x < 0.6$, $(KBr)_{1-x}(KCN)_x$ exhibits a low-temperature

glass state. In diffraction experiments the glass state is characterized by an anisotropic pattern of diffusive scattered intensities centered around the Bragg positions of the cubic lattice.[4,5,23]

The motivation of this investigation was to study the statics of the transition in (KBr):(KCN) near the critical concentration x_c, just on the borderline between elastic order and the glassy state. Using elastic neutron diffraction we studied $(KBr)_{0.35}(KCN)_{0.65}$ $(x > x_c)$ and $(KBr)_{0.43}(KCN)_{0.57}$ $(x < x_c)$ paying special attention to the temperature- and momentum-transfer dependence of the broadening of the diffraction lines. From recent specific-heat measurements,[19,29] we know that the specific-heat anomaly at the ferroelastic transition, which is strongly of first order in pure KCN, shows up just as a change of slope in $c_p(T)$ for $x = 0.65$ and exhibits no anomaly at the glass transition in $(KBr)_{0.43}(KCN)_{0.57}$. In both crystals the configurational entropy is smeared out over a wide temperature range and the c_p versus T curves look very similar. We expected that this similarity should also be displayed in the diffraction pattern.

In addition, there are a number of further questions we want to address in this study.

Recently it has been observed that the diffuse intensities plotted versus the wave vector q are not given by Lorentzian line shapes, as theoretically predicted,[5] but rather by an exponential q dependence. In this work we made therefore a detailed analysis of the line shapes.

Loidl et al.[23] reported a preliminary investigation of $(KBr)_{0.47}(KCN)_{0.53}$ where they claimed to find a crystalline to amorphous transition. This conclusion was drawn through an analysis of the Q-dependent broadening of the Bragg reflections in the glass state. However, a closer inspection of the data showed that this analysis was incorrect: at low Q values a Bragg spike on top of the diffusive scattered intensities could still be detected. Here we report a revised analysis.

There exists experimental evidence that the cubic to rhombohedral transition in $(KBr)_{1-x}(KCN)_x$ for concentrations $0.75 \lesssim x \lesssim 0.6$ is a second-order phase transition[3,29] with the elastic shear modulus tending continuously to zero. This complete softening of T_{2g} phonons which propagate within the cube planes should lead to a logarithmic divergence of the mean-square displacements of the ions. Therefore, we have attempted a rigorous structure factor analysis.

II. EXPERIMENTAL RESULTS

$(KBr)_{1-x}(KCN)_x$ single crystals with concentrations $x = 0.53$, 0.57, and 0.65 were investigated. The crystals have been grown by S. Haussühl at the Institut für Kristallographie at the University of Cologne. The elastic neutron-scattering experiments were carried out on the triple-axis spectrometer D10 located on a thermal neutron guide at the Institute Laue-Langevin in Grenoble. The samples were mounted on an Eulerian cradle to allow scanning along all reciprocal-lattice directions. A vertically focusing Cu(200) monochromator gave a wavelength of 1.260 Å. A He-flow cryostat[30] allowed varia-

tion of the temperature from 4 to 300 K with an accuracy of 0.1 K. In most of the scans the pyrolytic graphite analyzer was set at the (004) reflection to give an energy resolution of approximately 1.5 meV and was set to zero energy transfer. For $(KBr)_{0.47}(KCN)_{0.53}$ complete sets of reflections to $\sin\theta/\lambda = 0.68$ were also scanned in the diffractometric mode without the analyzer at 10, 99, and 295 K. At least three symmetry equivalents of each unique reflection were scanned. Unless otherwise stated the scans presented in the figures were obtained with the analyzer.

A. Results for $(KBr)_{0.47}(KCN)_{0.53}$

Figure 1 which also appeared in the earlier communication[23] presents scans through various reciprocal-lattice points at 10 K, a temperature which is far below the freezing temperature $T_F(THz) \simeq 100$ K.[23] All the scans shown are taken along the [010] direction in the (001) plane of the reciprocal lattice. These data imply a strong increase of the intrinsic linewidth with momentum transfer Q. The asymmetric contributions in the (420), (440), and (660) reflections can be explained by the theory of Michel and Rowe,[5] who formulated a neutron scattering law for orientational glasses. These authors found that in addition to the Bragg contributions, diffusive intensities appear, namely a symmetric Q^2/q^2 term and, depending on symmetry of the strain field, an
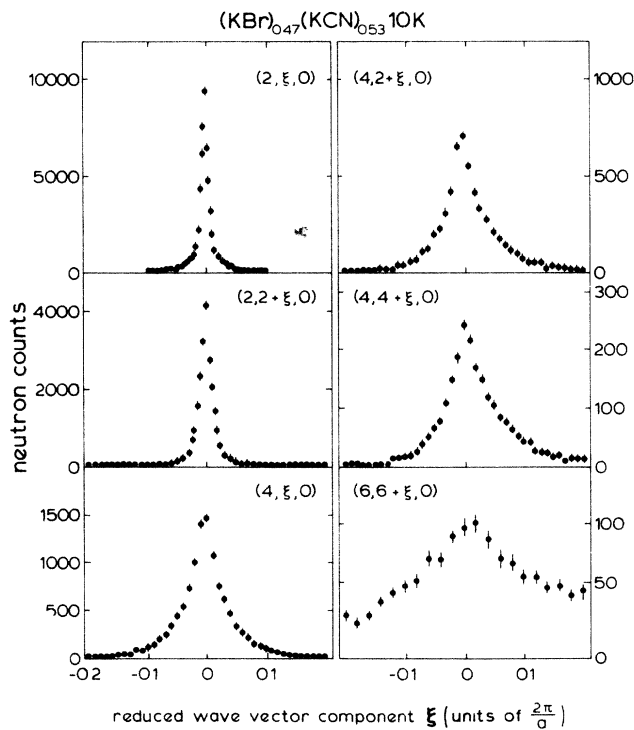

FIG. 1. Transverse scans at zero energy transfer in the (001) plane through various reciprocal-lattice points in $(KBr)_{0.47}(KCN)_{0.53}$ at 10 K. (Figure taken from Ref. 23 and reproduced with permission by courtesy of Pergamon Press.)
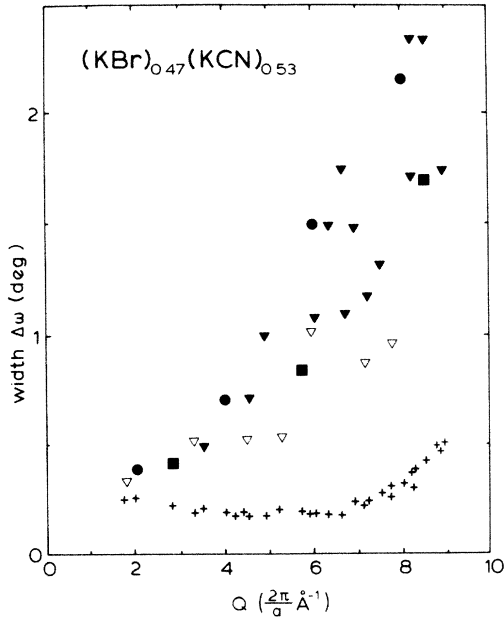
FIG. 2. The observed widths of neutron-diffraction rocking curves for the $(KBr)_{0.47}(KCN)_{0.53}$ single crystal as a function of the normalized scattering vector. The room-temperature data (+) reflect the mosaic spread of the crystal and the finite instrumental resolution. All the other symbols refer to measurements in the glass state at 10 K $[Q=(h^2+k^2+l^2)^{1/2}]$: solid symbols, (hkl) all even; open symbols, (hkl) all odd; $(h00)$, ●; $(hh0)$, ■; (hkl), ▼.

FIG. 3. Symmetrized line shapes $(q^++q^-)/2$ of various Bragg reflections in $(KBr)_{0.47}(KCN)_{0.53}$ at 10 K.

asymmetric Q/q term, where q is the phonon wave number.

The linewidths $\Delta\omega$ (deg) observed in the scans without the analyzer for all diffraction lines are plotted in Fig. 2 against momentum transfer for two temperatures: The widths of the room-temperature data are determined mainly by the resolution of the spectrometer. At 10 K the linewidths are dramatically increased. We also see from Fig. 2 that the broadening is anisotropic. Focusing on the reflections with (hkl) all even, the $(h00)$ reflections are most strongly affected, while the $(hh0)$ peaks are less broadened. This demonstrates that the frozen-in strain fields are of T_{2g} symmetry.[4,23]

The disagreement of the line shapes and the Q dependence of the linewidths with the present theories for orientational glasses prompted us to perform similar but more detailed experiments on samples of other concentrations near the critical concentration. In Ref. 23 the peaks observed in the scans made with the analyzer were fitted using a single Lorentzian line shape. In case of asymmetric peaks, the data were symmetrized by adding the intensities of the plus and the minus q values and then dividing by 2. This analysis gave an intrinsic linewidth $\Delta Q \propto Q^3$. However, closer inspection of the line shapes of Fig. 1, for example, shows significant deviations from a simple Lorentzian form and in addition, at low Q values, Bragg spikes above the diffusive intensities. To demonstrate this behavior, we plot the logarithm of the intensity I of the scans of Fig. 1 versus the reduced wave vector in Fig. 3. This clearly shows that
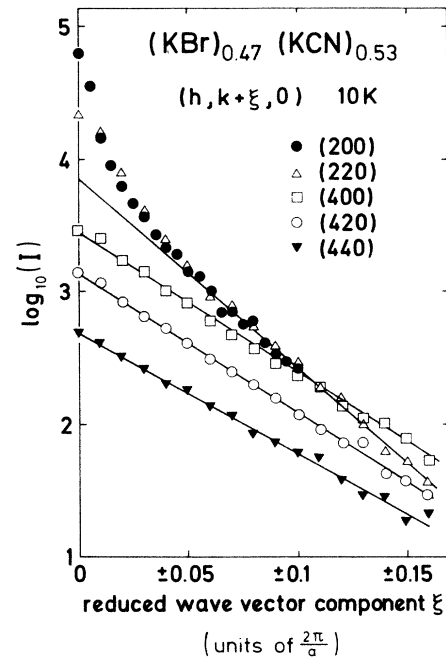
the lines shapes are of exponential form for high Q, while for low Q, a Bragg spike can still be detected above the diffuse intensities. From the existence of resolution-limited Bragg reflections, we conclude that $(KBr)_{0.47}(KCN)_{0.53}$ on the average is still a cubic crystal, characterized, however, by a large Debye-Waller factor due to frozen-in strain fields. A more detailed analysis of the temperature dependence of Bragg intensities and diffuse intensities will be presented for $(KBr)_{1-x}(KCN)_x$ crystals with concentrations $x = 0.57$ and 0.65.

B. Results in $(KBr)_{0.43}(KCN)_{0.57}$ and $(KBr)_{0.35}(KCN)_{0.65}$

In studying these crystals we intended to make a direct comparison of the statics of an orientational glass transition with the statics of a structural phase transition. In the former case we find a transformation from the high-temperature plastic phase into a glass state with frozen-in orientational correlations and frozen-in lattice strains; in the latter case the plastic is transformed into a low-temperature rhombohedral phase. Recent calorimetric experiments[29] have demonstrated that the c_p versus T curves look very similar for these two concentrations. In $(KBr)_{0.43}(KCN)_{0.57}$ the specific heat varies smoothly over the entire temperature range: for $x = 0.65$ the c_p curve exhibits a small anomaly, visible as a change of slope only.

In Fig. 4 we show transverse scans through the (060) reflection of $(KBr)_{0.43}(KCN)_{0.57}$ at various temperatures. At $T = 105$ K only a small thermal diffuse-scattering
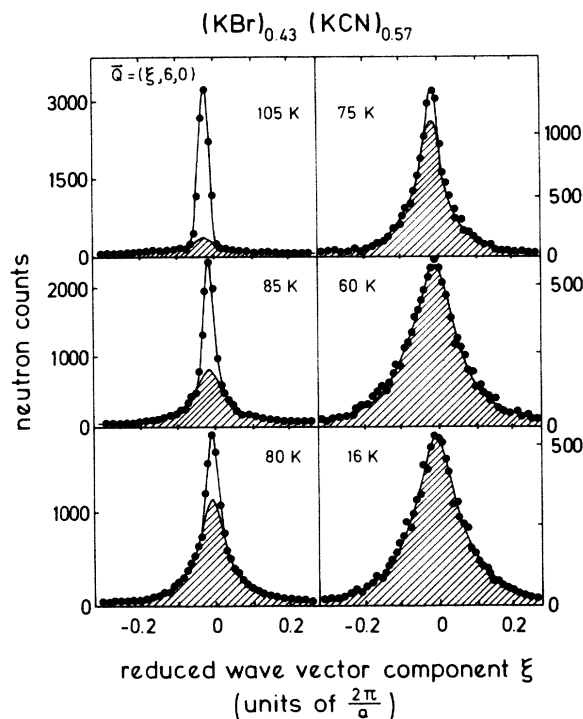
$(KBr)_{0.43}$ $(KCN)_{0.57}$

FIG. 4. Transverse scans at zero energy transfer through the (060) reflection in the (001) plane of $(KBr)_{0.43}(KCN)_{0.57}$ at various temperatures. The hatched area shows the diffuse contribution from the frozen-in strain fields, the empty peak the "true" Bragg intensity. The solid lines are the results of fits as explained in the text.

component is visible below a well-defined Bragg spike. With decreasing temperature the diffuse contributions increase while the Bragg scattering decreases. Below 70 K the Bragg contribution has vanished completely. Figure 5 illustrates the Q dependence of the ratio of Bragg and diffuse components at 16 K. Here transverse scans are shown for a series of $(0k0)$ reflections. We notice
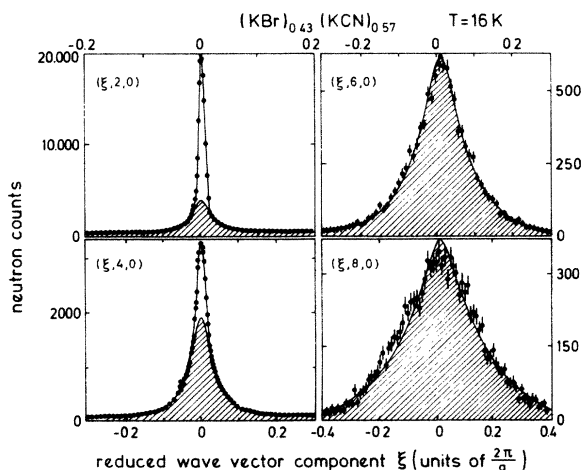

FIG. 5. Transverse scans through a series of $(0k0)$ reflections in $(KBr)_{0.43}(KCN)_{0.57}$ at 16 K. The hatched area shows the diffuse contribution from the frozen-in strain fields, the empty peak the "true" Bragg intensity. The solid lines are the results of fits as explained in the text.

that true Bragg scattering is visible only for $k \leq 4$. Obviously a very large Debye-Waller factor is responsible for this phenomenon whose static part is directly related to the intensities of the diffuse components. These static mean-square displacements are due to frozen-in random strains of T_{2g} symmetry.

Utilizing the theoretical approach by Michel and Rowe[25] the anisotropic pattern of diffuse scattered intensities can be described by a Q^2/q^2 dependence, and depending on the symmetry of the frozen-in strain field, by an asymmetric Q/q term. In $(KBr)_{1-x}(KCN)_x$ this asymmetry is easily detectable in scans of the type $(h+q,h,0)$ or $(h,h+q,0)$. To illustrate the asymmetry more quantitatively we calculated the symmetric contributions $[I(q^+)+I(q^-)]/2$, which should follow a $1/q^2$ law, and the asymmetric part of the peak, namely $[I(q^+)-I(q^-)]$, theoretically described by a $1/q$ dependence, for a series of $(hh0)$ reflections.

The results for the (220) and (660) reflections are shown in Fig. 6 in a semilogarithmic plot. The symmetric and asymmetric parts of the line shapes as measured at the (220) reflection are of equal intensity and, even more importantly, both can be described by a straight line with essentially the same slope. Obviously both contributions can be described by $I = I_0 e^{-\lambda q}$ with unique prefactor I_0 and coefficient λ. For small q values, Bragg scattering dominates the line shape. The results for the (660) reflection also indicate a logarithmic dependence of symmetric and asymmetric part of the diffuse scattered intensities. Again the slope for both contributions is the same but the prefactor of the antisymmetric part is a factor of 4 smaller than that of the symmetric part.

This exponential decay of the diffuse intensities can be found in all the $(0k0)$ transverse scans. It immediately suggests that higher-order terms in the phonon coordinates play an important role. However, at present there
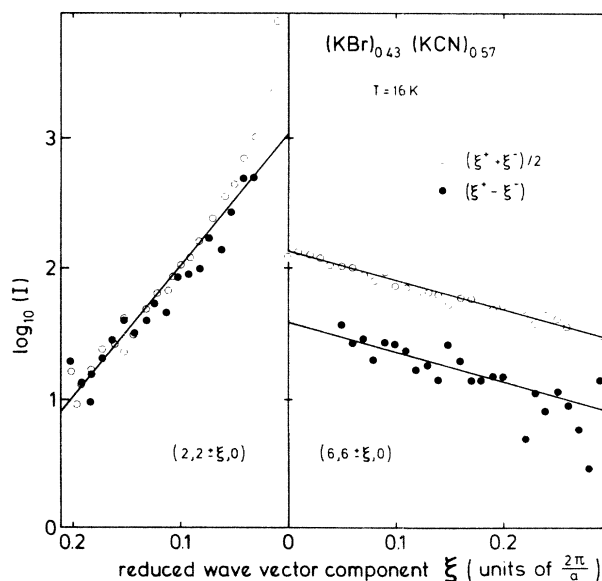

FIG. 6. Symmetrized and antisymmetrized line shapes of transverse scans through the (220) and (660) reflection in $(KBr)_{0.43}(KCN)_{0.57}$ at 16 K on a semilogarithmic scale.

is no theoretical approach that describes these unusual line shapes. Any reliable theory has also to explain the strong Q dependence of the coefficient α in the exponent and the behavior of symmetric and asymmetric contributions of the diffuse scattered intensities as mentioned above.

Similar results were obtained for $(KBr)_{0.35}(KCN)_{0.65}$. This crystal undergoes a structural phase transition at $T_s = 97.5$ K.[29] The temperature dependence of transverse scans through the (060) reflection is shown in Fig. 7. Between 110 and 97.5 K there is a rapid decrease of the Gaussian (Bragg) contribution. Near the structural phase transition the scattered intensities are predominantly diffuse. At T_s the peaks look very similar to those observed in $(KBr)_{0.43}(KCN)_{0.57}$ at low temperatures in the glass phase. Again the scattered intensities can be explained assuming a distribution of shear strains: at $T \simeq T_s$ the elastic shear constant c_{44} is almost completely soft.[3] c_{44} defines shear deformations within a plane rather than along a line, and a "melting transition" within the cube planes of the lattice is induced as c_{44} approaches 0, which in turn yields a divergence of the mean-square displacements.[31] For $T \lesssim T_s$ the free energy favors one well-defined rhombohedral distortion and with decreasing temperatures this homogeneous distortion is established and favored above a distribution of random shear strains. At low T the fraction of diffuse scattered intensities is strongly reduced.
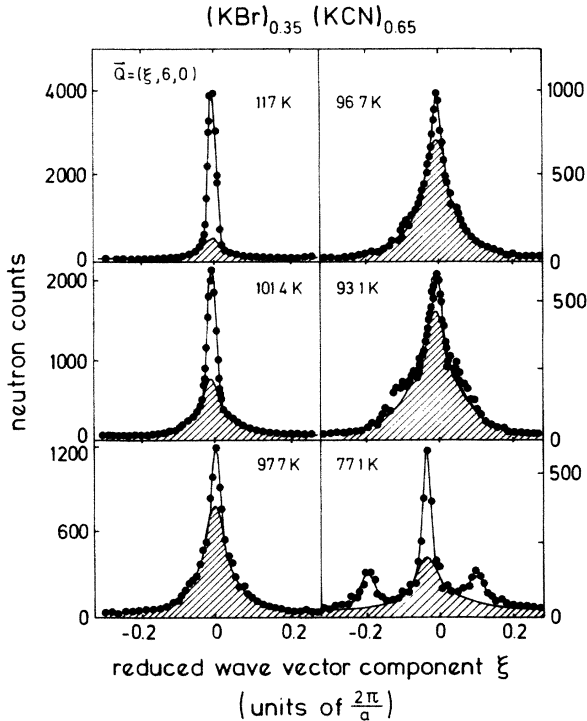

FIG. 7. Transverse scans at zero energy transfer through the (060) reflection in $(KBr)_{0.35}(KCN)_{0.65}$ at various temperatures. The cubic to orthorhombic phase transition takes place at 97.5 K. The shaded area shows the contribution from frozen-in shear strains, the empty area that from Bragg scattering; the solid lines represent the result of fits as explained in the text.

III. ANALYSIS OF THE RESULTS

In the present investigation of $(KBr)_{1-x}(KCN)_x$ mixed crystals two types of experiments have been performed. For $x = 0.53$ we presented a structure factor determination to determine the orientational distribution of the CN^- molecules. In the crystals with concentrations $x = 0.57$ and 0.65 we tried to analyze the temperature dependence of the diffuse and of the Bragg scattering contributions. This analysis should yield information concerning Debye-Waller factors, line shapes, and the freezing of coupled rotations and translations.

A. $(KBr)_{0.47}(KCN)_{0.53}$

The squared structure factors F_{hkl}^2 of $(KBr)_{0.47}(KCN)_{0.53}$ measured at 10, 99, and 295 K were used to determine the orientational distribution of the CN^- ions in these mixed molecular crystals. In the analysis we followed closely the model, suggested by Seymour and Pryor,[32] which has been used by Rowe et al.[33] to determine the angular distribution of the CN^- dumbbells in KCN and NaCN. The relevant parameters in this model are the expansion coefficients α_4 and α_6 of the fourth- and sixth-order spherical Bessel functions describing the angular distribution of the CN^- ions, the CN bond length d and the mean-square displacements $\langle u_{\kappa,\alpha}^2 \rangle$ of the center-of-mass lattice at the site κ. A model has also been developed[34] to include anisotropic center-of-mass displacements. This procedure introduces four new parameters, and in our case does not lead to a significantly better fit. For this reason we cite here the results with isotropic center-of-mass displacement, which can be compared directly to the results of Rowe et al.[33]

The structure factors of the reflections were found by summing the background-corrected counts observed in the coupled scans, when the background was assumed to be given by the nearly constant counts at the limits of each scan. Thirty-five independent Bragg reflections were used in the determination of the orientational distribution function. Some problems arose at $T = 10$ K. As can be seen from Fig. 1, at large Q values the peaks consist of diffuse intensities only. True Bragg scattering can be found at lowest Q values only. However, since the diffuse scattering, like any phonon scattering, is scaled by the Bragg peak, only the overall temperature factor will be in error. We also performed a similar analysis of structure factors from pure KCN.[34] In KCN the diffraction data were collected at 295 K and at 185 K just above the structural phase transition $T_s = 168$ K. Here 27 independent reflections could be collected. In this case all the intensities were corrected for thermal diffuse scattering.

This model of orientational distributions of the CN^- molecules takes into account large orientational fluctuations, but is restricted to harmonic contributions in the translational lattice. However, orientational relaxation processes imply large translational displacements and higher-order terms in the Q dependence of the Debye-Waller factors may become important. Therefore the present analysis of the structure factors in terms of har-

TABLE I. Parameters obtained from the analysis of the F_{hkl}^2 of KCN and of $(KBr)_{0.47}(KCN)_{0.53}$: the cubic harmonic coefficients α_4 and α_6; component α of the mean-square displacement at site κ ($\kappa \equiv K^+, CN^-/Br^-$), $\langle u_{\kappa,\alpha}^2 \rangle$; and the C—N bond length. The estimated uncertainties in parentheses correspond to fitting errors only.

CN⁻ concentration x	T (K)	Coefficient of cubics α_4	Coefficient of cubics α_6	C≡N bond length (Å)	$\langle u_{\kappa,\alpha}^2 \rangle$ (Å) K⁺	$\langle u_{\kappa,\alpha}^2 \rangle$ (Å) CN⁻/Br⁻
1	295	−0.201(21)	0.53(20)	1.177(2)	0.068(1)	0.066(2)
1	185	−0.066(25)	0.63(25)	1.182(3)	0.066(1)	0.058(2)
0.53	295	−0.070(23)	0.25(8)	1.174(2)	0.044(2)	0.037(3)
0.53	99	0.175(34)	0.30(10)	1.180(2)	0.037(2)	0.032(3)
0.53	10	0.360(36)	−0.08(6)	1.190(3)	0.057(4)	0.048(4)

monic mean-square displacements gives only a rough estimate concerning the T dependence of the distribution of molecular orientations.

The final parameters of these fits are given in Table I. From the expansion coefficients α_4 and α_6 we calculated the angular distribution of the CN⁻ orientations for KCN and for $(KBr)_{0.47}(KCN)_{0.53}$ (Fig. 8). For KCN the results are similar to the findings of Rowe et al.[33] The maximum probability for orientations of CN⁻ ions is along [111] while the [110] directions exhibit a minimum at all temperatures. For $(KBr)_{0.47}(KCN)_{0.53}$ the probability distribution for the molecular orientations is strongly temperature dependent. At room temperature the CN⁻ ions are oriented preferably along [111], closely resembling the orientation in pure KCN. But at 100 K and even more so at 10 K the maximum probability for CN⁻ orientations points along [100]. To investigate this effect in more detail we followed the temperature dependence of the Bragg intensities of the (551) and the (771) reflections which appear at the scattering angle 2Θ but involve very different scattering planes. In a model with an isotropic distribution of CN⁻ orientations these intensities should be the same. Figure 9 shows that they

are not. This figure nicely shows the combined effect of temperature-dependent changes of the angular CN⁻ distribution and of the temperature dependence of the Debye-Waller factors. Obviously at about 140 K the angular distribution changes, as can be seen from the ratio of the (551) and (711) Bragg intensities. The average mean-square displacement is approximately proportional to the sum of the intensities of the two reflections exhibits a minimum—corresponding to the maximum peak intensities—also at 140 K.

B. $(KBr)_{0.43}(KCN)_{0.57}$ and $(KBr)_{0.35}(KCN)_{0.65}$

In the analysis of the measurements in the crystals with CN⁻ concentrations $x = 0.57$ and 0.65, we separated the Gaussian Bragg contribution from the diffuse scattered intensities. The diffuse contributions were
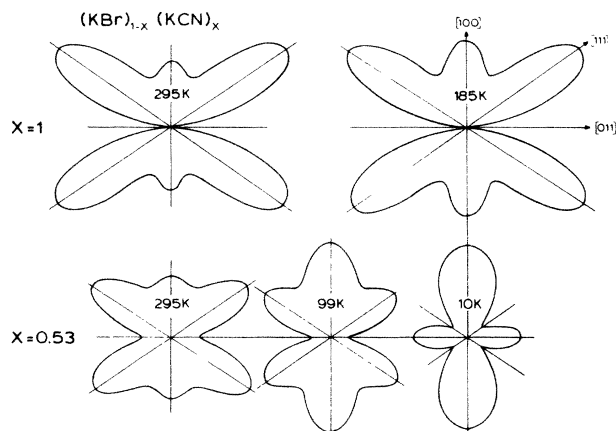

FIG. 8. The orientational distribution of the CN⁻ molecules in the (011) plane for KCN and for $(KBr)_{0.47}(KCN)_{0.53}$ at various temperatures. Note the increasing preference for orientation in the ⟨100⟩ directions with decreasing temperatures for both concentrations.
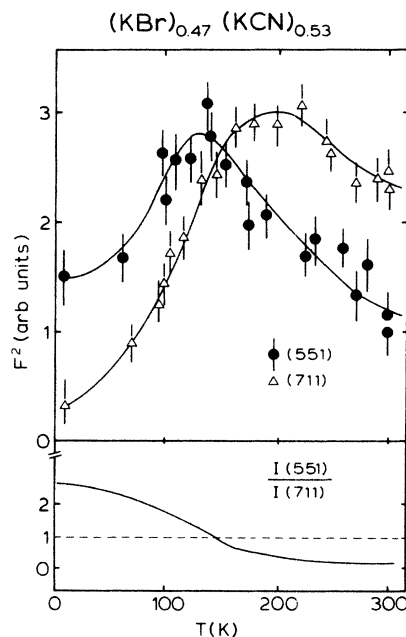

FIG. 9. Temperature dependence of the intensities of the (551) and (711) Bragg reflections for $(KBr)_{0.47}(KCN)_{0.53}$. The lower part gives the ratio of $I(551)/I(711)$.

fitted using an exponential profile of the form $I = I_0 \exp(-\alpha q)$. This gave a significantly better fit than a Lorentzian line shape. Only the symmetrized data of the $(hh0)$ reflections were analyzed. Representative results of these fits using a Gaussian line shape for the Bragg peaks and an exponential line shape folded with the experimental resolution for the diffuse intensities are shown as solid lines in Figs. 4, 5, and 7. From these fits we were able to determine the squared structure factors F^2_{hkl} for the reflections (hkl) as measured at different temperatures. The resulting $|F^2|$ as determined for the $(0k0)$ reflections in $(KBr)_{0.43}(KCN)_{0.57}$ and $(KBr)_{0.35}(KCN)_{0.65}$ are shown in Figs. 10 and 11, respectively. In both crystals all F_{hkl} strongly decrease with decreasing temperatures for $T \lesssim 100$ K. This indicates a strong increase of the mean-square displacements with decreasing temperatures, contrary to the behavior of a normal anharmonic crystal. For $x = 0.57$ the intensities of the Bragg reflection stay constant at temperatures below 70 K. At this temperature the freezing-in of shear strains is terminated.

A similar strong increase in the mean-square displacements is observed for $x = 0.65$. This crystal undergoes a structural phase transition into a rhombohedral low-temperature phase at $T_s = 97.5$ K. Already at $T > T_s$ the (060) and (080) reflections are undetectably small. But even at $T \simeq T_s$ the (020) and the (040) reflections are still observable.

For both crystals we therefore find no real divergence of the Debye-Waller factors. This is consistent with the x-ray diffraction profiles as measured in $(KBr)_{0.47}(KCN)_{0.53}$.[24] The mean-square displacements which are derived from this analysis are shown in Fig. 12 for $x = 0.57$ and 0.65. (The analyzer introduces a monotonic $|Q|$-dependent modification of the observed F^2_{hkl} which will lead to an error in the refined values of the overall mean-square displacement. This effect is not so severe, as can be seen by comparing the room-
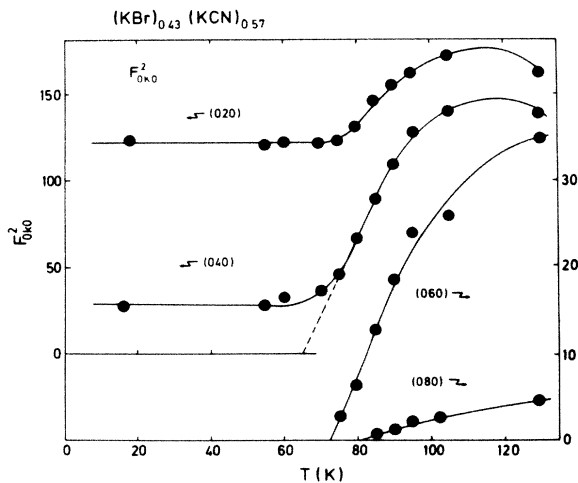
temperature $\langle u^2 \rangle$ values of Fig. 12 with those of Table I.) For $x = 0.57$ we find a strong increase for $T \geq 65$ K, and below that temperature a saturation, while for $x = 0.56$ we find an even more dramatic increase for $T \to T_s$ in $x = 0.65$. The latter result is in good agreement with recent molecular-dynamics simulations.[12]

For both crystals it is possible to define the temperature where the Debye-Waller factor would diverge: a linear extrapolation of $|F^2|$ as indicated by the dashed lines in Figs. 10 and 11 defines the temperature $\tilde{T}$ where the different $(0k0)$ and $(hh0)$ nodes would vanish. The results are shown in the Figs. 13 and 14 for $x = 0.57$ and 0.65, respectively. Within the error bars the $\tilde{T}$ values versus the wave vectors Q for $x = 0.65$ define a straight line yielding the temperature where the (000) reflection vanishes. It is at this temperature that the mean-square displacements would diverge. From Fig. 14 it is 90 K for $(KBr)_{0.35}(KCN)_{0.65}$, 7 °C below the phase transition.

FIG. 11. Temperature dependence of the squared structure factors F^2_{0k0} in $(KBr)_{0.35}(KCN)_{0.65}$.

FIG. 10. Temperature dependence of the squared structure factors F^2_{0k0} for a series of $(0k0)$ reflections in $(KBr)_{0.43}(KCN)_{0.57}$.

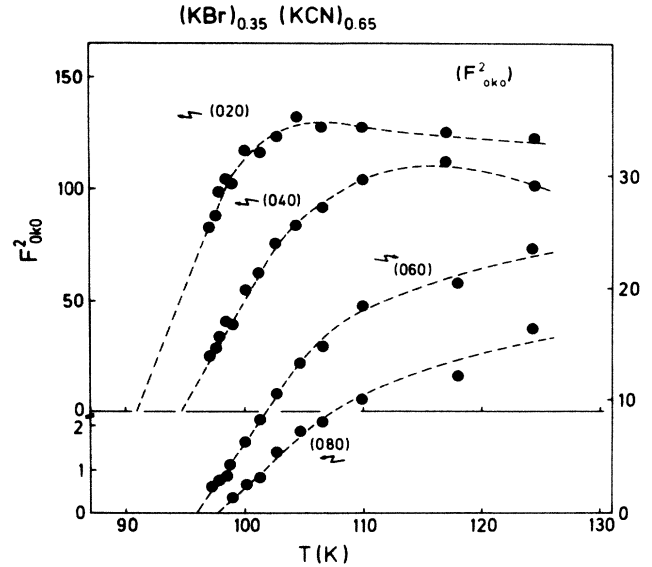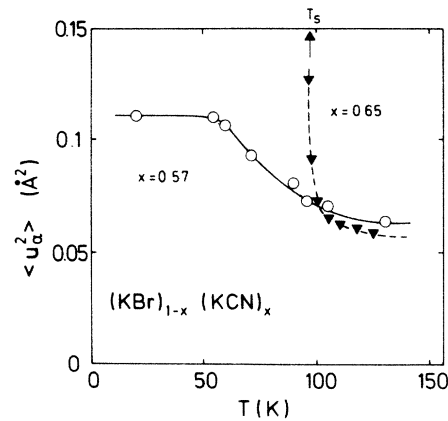FIG. 12. Temperature dependence of the mean-square displacements in $(KBr)_{1-x}(KCN)_x$ for concentrations $x = 0.57$ and 0.65.
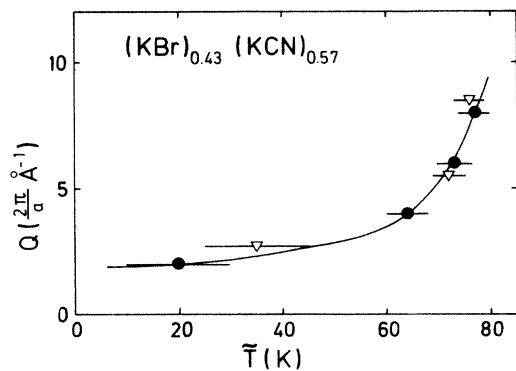
FIG. 13. Temperatures $\tilde{T}$ where the $(0k0)$ (●) and $(hh0)$ (△) nodes vanish or extrapolate to zero in $(KBr)_{0.43}(KCN)_{0.57}$.

For $x = 0.57$ the $\tilde{T}$ values indicate the saturation of the freezing process.

Finally, we analyzed the linewidth of the diffuse scattered intensities to gain insight into the statics of the orientational glass transition and of the structural phase transformation. The resulting linewidths ΔQ (half width at half maximum in units of the reciprocal lattice) versus the momentum transfer Q are shown in the Figs. 15 and 16 for $(KBr)_{0.43}(KCN)_{0.57}$ and $(KBr)_{0.35}(KCN)_{0.65}$, respectively. Both concentrations have $\Delta Q \propto Q$ above the transition temperature. However, for $x = 0.65$ long-range order is established below the structural phase transition temperature, while for $x = 0.57$ anomalies in the Q-dependent broadening become apparent below the glass transition temperature. The ordering compound $x = 0.65$ exhibits a linewidth that increases linearly with Q ($\Delta Q \propto Q$) at all $T \gtrsim T_s$. This effect can be explained in terms of an inhomogeneous strain broadening; for instance, a distribution of shear distortions would yield such a diffraction pattern.

The linewidth effects in $(KBr)_{0.43}(KCN)_{0.57}$ are much more complex. Again for $T \gtrsim 70$ K ΔQ increases linearly with Q. This is the temperature region where the Debye-Waller factor still increases with decreasing temperatures. However, for $T \lesssim 70$ K where the mean-square displacements become independent of temperature and for high Q values significant deviations from this linear behavior become apparent.
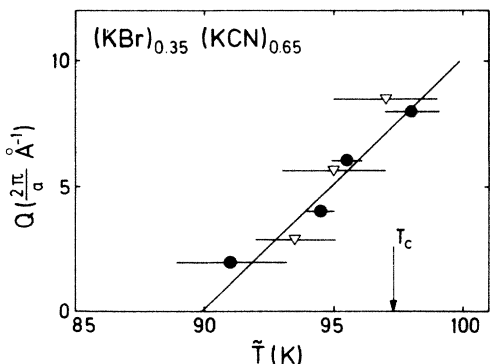

FIG. 14. Temperatures $\tilde{T}$ where the $(0k0)$ (●) and the $(hh0)$ (△) nodes in $(KBr)_{0.35}(KCN)_{0.65}$ vanish or extrapolate to zero.
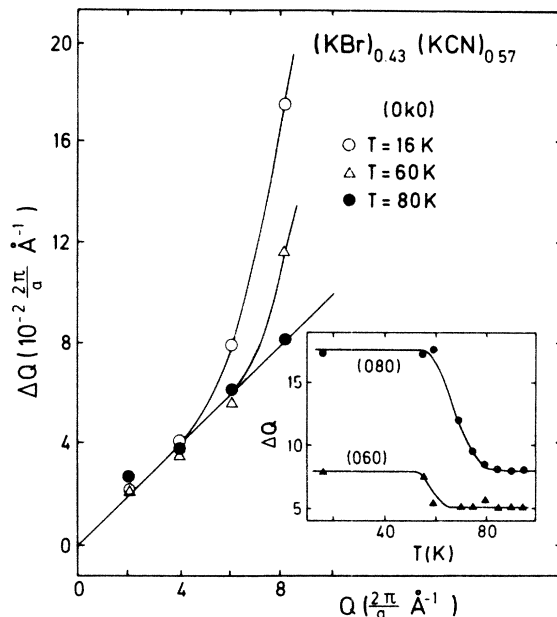

FIG. 15. Half width at half maximum ΔQ of the diffuse scattered intensities at different temperatures in $(KBr)_{0.43}(KCN)_{0.57}$. Note the strong deviations from a linear Q dependence as expected for a broadening due to random strains for temperature $T \lesssim 70$ K. The inset shows the temperature dependence of ΔQ for the (060) and (080) reflections. The lines are drawn to guide the eye.

IV. DISCUSSION AND CONCLUDING REMARKS

The most relevant results of this single-crystal neutron-diffraction study in $(KBr)_{1-x}(KCN)_x$ are the following.

(i) The influence of the lattice-mediated interactions on the single-particle potential. It has been shown theoretically by Michel and Rowe[35] that the single-particle po-
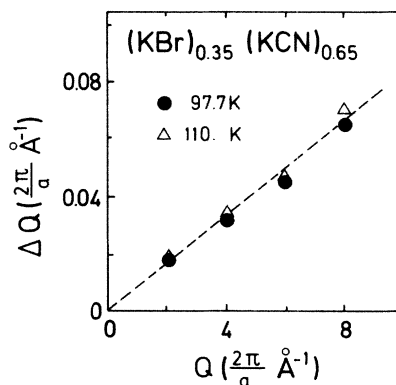

FIG. 16. Half widths at half maximum ΔQ of the diffuse intensities versus momentum transfer Q in $(KBr)_{0.35}(KCN)_{0.65}$ at 97.7 and 110 K.

tential of the crystal field as seen by the CN^- ions is strongly modified due to the rotation-translation coupling. In particular the self-interaction combined with deviations of the CN^- ion from centrosymmetry gives a temperature-dependent orientational potential favoring local maxima in $\langle 100 \rangle$ directions with decreasing temperatures. We have experimentally verified this behavior in $(KBr)_{0.47}(KCN)_{0.53}$. For temperatures $T \lesssim 140$ K the CN^- ions are aligned with highest probability along $\langle 100 \rangle$, which demonstrates the increasing importance of strain-mediated interactions. At higher temperatures, the CN^- ions are aligned with highest probability along $\langle 111 \rangle$, similar to the findings for very dilute KBr:CN crystals.[19] At these temperatures the single-particle potential dominates the orientational distribution of the CN^- ions.

(ii) The freezing-in of orientational and translational modes. The main aim of the present study was to study the statics of the orientational glass and to follow the freezing-in of translational modes coupled to orientational correlations. We also wanted to compare the statics of the orientational glass state to the statics of a structural ferroelastic phase transition, as occurs in $(KBr)_{1-x}(KCN)_x$ just above the critical concentration $x_c \simeq 0.6$. Obviously both transitions are characterized by a delicate balance between the rotation-translation coupling and the coupling of rotational modes to random strains as proposed by Lewis and Klein.[12] The random strains are generated by the substitutional Br^- atoms which act as static impurity centers. The effect of increasing Br^- concentrations $(1-x)$ is twofold: it leads to a reduction of the ferroelastic phase transition via a decrease of the rotation-translation coupling while at the same time it increases the random strain-rotation coupling. For concentrations $x \lesssim 0.6$ the latter suppresses the structural transition and causes the freezing into an orientational glass state. The characteristic feature of the orientational glass is the appearance of diffuse scattered intensities around reciprocal-lattice points. For $x \gtrsim 0.6$, the rotation-translation coupling still dominates over the random strain-rotation coupling and drives a ferroelastic phase transition. However, the large diffuse intensities due to frozen-in shear strains at temperatures just above T_s show the importance of the strain-rotation coupling even in the ordering systems.

It seems that the phase transition temperature in $(KBr)_{0.35}(KCN)_{0.65}$ can be defined as in systems with a percolation limit: at T_s, regions of one characteristic shear distortion are connected yielding an infinite "backbone" of elastic order. The regions exhibiting different shear distortions are continuously reduced in favor of this well-defined distortion. This result immediately ex-

plains the "third-order" character of the specific-heat anomaly, visible only as a change of slope in the c_p versus T curves.[29] The additional entropy at T_s to establish long-range order is negligible. The increase and the decrease of the diffuse intensities are a direct measure of the smearing out of the configurational entropy over a wide temperature range from far above to far below T_s.

At the orientational glass transition the distribution of shear strains is frozen-in and the specific heat is smooth down to the lowest temperatures.

(iii) Anomalous temperature dependence of the Debye-Waller factors. Both crystals investigated $(x = 0.57$ and $0.65)$ exhibit an anomalous temperature dependence of the mean-square displacements. At high T $(x = 0.65,\ T \gtrsim T_s;\ x = 0.57,\ T \gtrsim 70$ K$)$ this is due to a softening of the elastic shear modes. For $(KBr)_{0.43}(KCN)_{0.57}$ and $T \lesssim 70$ K the large Debye-Waller factors can be explained due to frozen-in orientational and translational modes. This behavior is in excellent agreement with theoretical results[35] and with molecular-dynamics simulations.[12]

(iv) The linewidth of the diffuse scattered intensities. The momentum-transfer dependence of the linewidth of the diffuse intensities can be divided into two regions: in a high-temperature regime $(x = 0.65,\ T \gtrsim T_s;\ x = 0.57,\ T \gtrsim 70$ K$)$ the linewidth ΔQ depends linearly on the momentum transfer Q. This observation can be interpreted as being the result of a distribution of shear strains of T_{2g} symmetry centered around zero strain, or equivalently, by a distribution of local shear deformations of the cubic lattice. For $T \lesssim T_s$ and in $(KBr)_{0.35}(KCN)_{0.65}$ these local shear deformations are reduced in favor of one unique rhombohedral distortion exhibiting long-range order. In $(KBr)_{0.43}(KCN)_{0.57}$ and for temperatures $T \lesssim 70$ K we find significant deviations from the linear Q dependence of ΔQ. At present we have no explanation for this finding.

Finally, we would like to mention that as observed by Knorr and Loidl on x-ray data,[24] the line shapes of the diffuse scattered intensities follow an exponential behavior. We confirmed that the symmetric and the asymmetric parts of the diffuse intensities can be described using exponential line shapes. These line shapes cannot be explained within existing theories.[5]

ACKNOWLEDGMENTS

[1] K. H. Michel and J. Naudts, Phys. Rev. Lett. **39**, 212 (1977).

[2] J. M. Rowe, J. J. Rush, N. J. Chesser, K. H. Michel, and J. Naudts, Phys. Rev. Lett. **40**, 455 (1978).

[3] K. Knorr, A. Loidl, and J. K. Kjems, Phys. Rev. Lett. **55**, 2445 (1985).

[4] J. M. Rowe, J. J. Rush, D. J. Hinks, and S. Susman, Phys. Rev. Lett. **43**, 1158 (1979).

[5] K. H. Michel and J. M. Rowe, Phys. Rev. B **22**, 1417 (1980).

[6] A. Loidl, R. Feile, and K. Knorr, Phys. Rev. Lett. **48**, 1263 (1982).

[7] J. M. Rowe, J. J. Rush, and S. Susman, Phys. Rev. B **28**, 3506 (1983).

[8] K. Knorr and A. Loidl, Phys. Rev. B **31**, 5387 (1985).

[9] S. Elschner, K. Knorr, and A. Loidl, Z. Phys. B **61**, 209

(1985).

[10]J. M. Rowe, J. Bouillot, J. J. Rush, and F. Lüty, Physica 136B, 498 (1986).

[11]S. Haussühl, Solid State Commun. 13, 147 (1973).

[12]L. J. Lewis and M. L. Klein, Phys. Rev. Lett. 57, 2698 (1986).

[13]K. H. Michel, Phys. Rev. Lett. 57, 2188 (1986); Phys. Rev. B 35, 1405 (1987); 35, 1414 (1987).

[14]S. K. Satija and C. H. Wang, Solid State Commun. 28, 617 (1978).

[15]A. Loidl, R. Feile, and K. Knorr, Z. Phys. B 42, 143 (1981).

[16]C. W. Garland, J. Z. Kwiecien, and J. C. Damien, Phys. Rev. B 25, 5818 (1982).

[17]R. Feile, A. Loidl, and K. Knorr, Phys. Rev. B 26, 6875 (1982).

[18]K. Knorr, U. G. Volkmann, and A. Loidl, Phys. Rev. Lett. 57, 2544 (1986).

[19]F. Lüty, in Defects in Insulating Crystals, edited by V. M. Turkevich and K. K. Svarts (Springer-Verlag, Berlin, 1981).

[20]S. Bhattacharya, S. R. Nagel, L. Fleishmann, and S. Susman, Phys. Rev. Lett. 48, 1267 (1982).

[21]U. G. Volkmann, R. Böhmer, A. Loidl, K. Knorr, U. T. Höchli, and S. Haussühl, Phys. Rev. Lett. 56, 1716 (1986).

[22]M. A. Doverspike, M.-C. Wu, and M. S. Conradi, Phys. Rev. Lett. 56, 2284 (1986).

[23]A. Loidl, M. Müllner, G. J. McIntyre, K. Knorr, and H. Jex, Solid State Commun. 54, 367 (1985).

[24]K. Knorr and A. Loidl, Phys. Rev. Lett. 57, 460 (1986).

[25]For a review see J. J. DeYoreo, W. Knaak, M. Meissner, and R. O. Pohl, Phys. Rev. B 34, 8828 (1986).

[26]J. F. Berret, P. Doussineau, A. Levelut, M. Meissner, and W. Schön, Phys. Rev. Lett. 55, 2013 (1985).

[27]D. Moy, J. N. Dobbs, and A. C. Anderson, Phys. Rev. B 29, 2160 (1984).

[28]J. M. Rowe, J. J. Rush, and E. Prince, J. Chem. Phys. 66, 5147 (1977).

[29]B. Mertz and A. Loidl, Europhys. Lett. 4, 583 (1987).

[30]C. M. E. Zeyen, R. Chagnon, F. Disdier, and H. Morin, Rev. Phys. Appl. 19, 789 (1984).

[31]R. Folk, H. Iro, and F. Schwabl, Z. Phys. B 25, 69 (1976); Phys. Rev. B 20, 1229 (1977).

[32]R. S. Seymour and A. W. Prior, Acta Cryst. B 26, 1487 (1970).

[33]J. M. Rowe, D. G. Hinks, D. L. Prince, S. Susman, and J. J. Rush, J. Chem. Phys. 58, 2039 (1973).

[34]U. Sievers, G. Heger, A. Loidl, and K. Knorr (unpublished).

[35]K. H. Michel and J. M. Rowe, Phys. Rev. B 32, 5827 (1985).